# Coherence generation and population transfer in a three-level ladder system*

Zhang Bing(张 冰)[a)b)c)d)], Jiang Yun(姜 云)[a)b)], Wang Gang(王 刚)[a)b)], Zhang Li-Da(张理达)[a)b)], Wu Jin-Hui(吴金辉)[a)b)], and Gao Jin-Yue(高锦岳)[a)b)†]

[a)] *College of Physics, Jilin University, Changchun* 130023, *China*

[b)] *Key Laboratory of Coherent Light and Atomic and Molecular Spectroscopy of Educational Ministry, Changchun* 130023, *China*

[c)] *College of Physics and Electronic Engineering, Mudanjiang Teachers' College, Mudanjiang* 157012, *China*

[d)] *Heilongjiang Superhard Materials Key Laboratory, Mudanjiang* 157012, *China*

(Received 3 September 2010; revised manuscript received 17 January 2011)

This work explores the effect of spontaneous emission on coherence generation and population transfer in a three-level ladder atomic system driven by two pulses in counterintuitive order. With adiabatic evolution and the weak-dephasing approximation, we find that a large coherence and population transfer can be achieved even with spontaneous decay rate. The maximum coherence and population transfer decrease with the increase of spontaneous decay rate from the highest state to intermediate state. But this effect can be compensated by shortening the pulse width and enlarging the delay time. Results show that the coherence generation and population transfer never depend on the spontaneous decay rate from the intermediate state to ground state. The validity of the analytic solution is examined by numerical calculation.

**Keywords:** coherence, population transfer, spontaneous decay

**PACS:** 03.65.–w, 42.50.–p, 42.50.Gy, 42.55.Ah **DOI:** 10.1088/1674-1056/20/5/050304

## 1. Introduction

Monochromatic coherent light delivers numerous advantages compared with broadband incoherent light. For instance, the possibility of completing efficient population transfer and coherence generation between discrete levels, which often shows intriguing counterintuitive features[1−12] and has potential applications in many aspects, such as the control of slow light dynamics,[2−5] frequency conversion on resonance[6,7] and all-optical logic operations.[13−15] One of the most efficient coherent excitation techniques is known as stimulated Raman adiabatic passage (STIRAP),[1,16−18] which is best explored in Λ-type atomic systems with two stable ground states (one acts as the initial state while the other is the target state) and one unstable intermediate state. A unique and fascinating feature of STIRAP is that the intermediate state, whose presence is crucial for providing two strongly coupled single-photon transitions, never gets populated, so that dynamical evolutions of atomic population and coherence are independent of the spontaneous decay of the intermediate state. Adiabatic population transfer between two quantum states can also be realized with chirped pulses,[19−22] which is equally efficient as STIRAP but usually applied to different situations.

Recently, significant attention has been paid to coherent population transfer in ladder-type atomic systems with only one stable ground state (the initial state) because of its importance in attaining short wavelength lasers, quantum logic gates based on dipole blockade, etc. Some relevant works have been implemented by several groups[23−29] with distinct focuses and purposes. Both intermediate and target states in ladder systems of real atoms and molecules are usually exposed to manifold decoherence effects, such as population decay due to spontaneous emission and pure phase relaxation due to inelastic atomic collisions. So, in principle, it is difficult to attain a perfect STIRAP in real atoms and molecules for a ladder configuration system.

With STIRAP in a lambda system, Ivanov *et al.* explored the effect of phase relaxation on the popu-

*Project supported by the National Natural Science Foundation of China (Grant No. 10774059), the National Basic Research Program of China (Grant No. 2006CB921101), and the Natural Science Foundation of Heilongjiang Province, China (Grant No. F200928).

†Corresponding author. E-mail: jygao@mail.jlu.edu.cn

© 2011 Chinese Physical Society and IOP Publishing Ltd

lation transfer efficiency in Ref. [30], and presented an analytical description where the target state did not decay to other states in Ref. [31]. Although the equations in the ladder system are similar to that in the lambda system, the essential difference between them is that the target state is the exciting state in a ladder system but is the ground state in a lambda system. The goal of this work is to analyse, from a general viewpoint, the population dynamics and coherence evolution of a three-level ladder system driven by two laser pulses (one pump and one Stokes), where spontaneous emission plays an important role and the adiabaticity[32] is not completely satisfied. In the adiabatic evolution and weak dephasing approximations,[30,31] we carried out detailed discussions with analytical solutions, which shows that spontaneous emission from the target state to the intermediate state is not an insuperable obstacle for achieving optimal coherence generation and efficient population transfer in the time region of interest. In addition, coherence generation and population transfer are almost irrelevant to spontaneous emission from the intermediate state to the ground state, which is a symbol of STIRAP. Except for the spontaneous decay rate of the target state, pulse width and time delay between the pump and coupling lasers are also critical for achieving the desired coherence generation and population transfer and thus should be carefully modulated. Finally, we would like to stress that our approximate analytical solutions have been checked by full numerical calculations.

## 2. Model, equations and analytical solutions

The model of a coherently driven three-level ladder system is illustrated in Fig. 1(a). The ground state $|1\rangle$ and the intermediate state $|2\rangle$ are connected by a pump laser of frequency $\omega_{\rm p}$ while the intermediate state $|2\rangle$ and the target state $|3\rangle$ are connected by a Stokes laser of frequency $\omega_{\rm s}$. The pump laser is detuned from the $|1\rangle \leftrightarrow |2\rangle$ transition by $\Delta_2 = \omega_{21} - \omega_{\rm p}$ while the Stokes laser is detuned from the $|2\rangle \leftrightarrow |3\rangle$ transition by $\Delta_3 = \omega_{32} - \omega_{\rm s}$. $\Gamma_{21}$ and $\Gamma_{32}$ describe the spontaneous emission rates from level $|2\rangle$ to level $|1\rangle$ and from level $|3\rangle$ to level $|2\rangle$, respectively.

Within the framework of the semiclassical theory, under the electric-dipole approximation and the rotating-wave approximation, we can represent the Hamiltonian in the interaction picture as

$$H_{\rm I} = \hbar[\Delta_2|2\rangle\langle 2| + (\Delta_2 + \Delta_3)|3\rangle\langle 3|] - \hbar[\Omega_{\rm p}|2\rangle\langle 1| + \Omega_{\rm s}|3\rangle\langle 2| + {\rm c.c.}], \quad (1)$$

where $\Omega_{\rm p} = d_{12}E_{\rm p}/2\hbar$ and $\Omega_{\rm s} = d_{23}E_{\rm s}/2\hbar$ are Rabi frequencies of the pump and Stokes lasers, respectively. For the purpose of efficient coherence generation between $|3\rangle$ and $|1\rangle$ and population transfer from $|1\rangle$ to $|3\rangle$, in the following, both pump and Stokes lasers are assumed to be Gaussian pulses in the time domain. In this case, the two Rabi frequencies may be described by $\Omega_{\rm p}(t) = \Omega_{\rm p0}{\rm e}^{-(t-\frac{\tau}{2})^2/T^2}$ and $\Omega_{\rm s}(t) = \Omega_{\rm s0}{\rm e}^{-(t+\frac{\tau}{2})^2/T^2}$ with $\tau$ being the time delay between the pump and Stokes pulses and $T$ being the widths of both pulses. Note that the pump and Stokes pulses are applied in counterintuitive order (i.e., the Stokes pulse precedes the pump pulse) when $\tau > 0$ [see Fig. 1(b)].

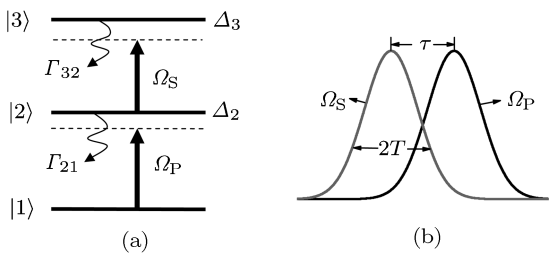



**Fig. 1.** (a) Energy-level diagram of a ladder-type atomic system with Rabi frequencies of $\Omega_{\rm p}$ (pump laser) and $\Omega_{\rm s}$ (Stokes lasers), respectively; (b) sketch map of the pump and Stokes pulses applied in counterintuitive order.

The master equation of motion for the density operator in an arbitrary multilevel atomic system is usually written as

$$\mathrm{i}\,\hbar\frac{\partial\rho}{\partial t} = [H_{\rm I}, \rho] + D, \quad (2)$$

where $D = -\frac{1}{2}\,\mathrm{i}\,\hbar\{\Gamma, \rho\}$ describes all irreversiable decoherence and depopulation processes. Starting from Eq. (1) and Eq. (2), it is straightforward to arrive at the following Liouville equations

$$\begin{aligned}
\dot\rho_{11} &= \Gamma_{21}\rho_{22} - \mathrm{i}\,\Omega_{\rm p}\rho_{12} + \mathrm{i}\,\Omega_{\rm p}^*\rho_{21},\\
\dot\rho_{22} &= -\Gamma_{21}\rho_{22} + \Gamma_{32}\rho_{33} + \mathrm{i}\,\Omega_{\rm p}\rho_{12}\\
&\quad - \mathrm{i}\,\Omega_{\rm p}^*\rho_{21} - \mathrm{i}\,\Omega_{\rm s}\rho_{23} + \mathrm{i}\,\Omega_{\rm s}^*\rho_{32},\\
\dot\rho_{33} &= -\Gamma_{32}\rho_{33} + \mathrm{i}\,\Omega_{\rm s}\rho_{23} - \mathrm{i}\,\Omega_{\rm s}^*\rho_{32},\\
\dot\rho_{12} &= -(\gamma_{12} - \mathrm{i}\,\Delta_2)\rho_{12} - \mathrm{i}\,\Omega_{\rm p}^*(\rho_{11} - \rho_{22}) - \mathrm{i}\,\Omega_{\rm s}\rho_{13},\\
\dot\rho_{13} &= -[\gamma_{13} - \mathrm{i}(\Delta_2 + \Delta_3)]\rho_{13} + \mathrm{i}\,\Omega_{\rm p}^*\rho_{23} - \mathrm{i}\,\Omega_{\rm s}^*\rho_{12},\\
\dot\rho_{23} &= -(\gamma_{23} - \mathrm{i}\,\Delta_3)\rho_{23} + \mathrm{i}\,\Omega_{\rm p}\rho_{13}\\
&\quad + \mathrm{i}\,\Omega_{\rm s}^*(\rho_{33} - \rho_{22}), \quad (3)
\end{aligned}$$

with $\gamma_{12} = \frac{1}{2}\Gamma_{21}$, $\gamma_{23} = \frac{1}{2}\Gamma_{32}$, $\gamma_{13} = \frac{1}{2}(\Gamma_{21} + \Gamma_{32})$ and constrained by $\rho_{ij} = \rho_{ji}$, ${\rm Tr}(\rho) = 1$. It is hard to directly obtain time-dependent analytical solutions for atomic coherences $\rho_{ij}$ and populations $\rho_{ii}$ from Eq. (3) by hand. To analytically solve Eq. (3), we transform

it from the diabatic basis $\rho = \{\rho_{ij}\}$ with $(i, j = 1, 2, 3)$ to the adiabatic basis $\rho^\alpha = \{\rho_{\mu\nu}\}$ with $(\mu, \nu = +, 0, -)$ as in Ref. [30]

$$\rho^\alpha = \boldsymbol{W}^{\mathrm{T}} \rho \boldsymbol{W}, \tag{4}$$

where $\boldsymbol{W}$ $(\boldsymbol{W}^{\mathrm{T}} = \boldsymbol{W}^{-1})$ is a rotation matrix

$$\boldsymbol{W}(\theta, \varphi) = \begin{pmatrix} \sin\theta\sin\varphi & \cos\varphi & \sin\theta\cos\varphi \\ \cos\varphi & 0 & -\sin\varphi \\ \cos\theta\sin\varphi & -\sin\theta & \cos\theta\cos\varphi \end{pmatrix} \tag{5}$$

derived from Eq. (1) in the absence of spontaneous decays. In Eq. (5), the mixing angles $\theta$ and $\varphi$ are defined as

$$\tan\theta(t) = \frac{\Omega_{\mathrm{p}}(t)}{\Omega_{\mathrm{s}}(t)}, \tan(2\varphi) = \frac{\Omega(t)}{\Delta_2 + \Delta_3}, \tag{6}$$

restricted in the adiabatic limit by $\Delta_2 + \Delta_3 = 0$ and $\Omega(t) = \sqrt{\Omega_{\mathrm{p}}^2(t) + \Omega_{\mathrm{s}}^2(t)}$. It is clear that we have $\varphi \equiv \frac{\pi}{4}$ under the two photon resonance condition of $\Delta_2 + \Delta_3 = 0$.

The master equation of motion for the density operator in the adiabatic basis reads

$$\mathrm{i}\,\hbar \frac{\partial \rho^\alpha}{\partial t} = [H^\alpha, \rho^\alpha] + \left[\boldsymbol{W}^{\mathrm{T}} \frac{\partial \boldsymbol{W}}{\partial t}, \rho^\alpha\right] + \boldsymbol{W}^{\mathrm{T}} D \boldsymbol{W}. \tag{7}$$

The adiabatic evolution of $\rho^\alpha$ in fact requires two necessary conditions: 1) the pump and Stokes pulses should be strong enough so that $\Omega_{\mathrm{p0,s0}} T \gg 1$;[28,30] 2) the two pulses should have an appropriate time delay so that $\tau \geq T(\sqrt{2} - 1)$ when $\tau/T < 1$ and

$$\frac{\tau}{T} \leq 2\sqrt{\ln\left(\frac{\Omega_0 T}{\pi}\right) - \frac{1}{2}\ln\left(4\ln\left(\frac{\Omega_0 T}{2\pi}\right)\right) - \cdots}$$

when $\tau/T > 1$.[30] In the limit of adiabatic evolution, we have indeed

$$\lim_{t\to-\infty} \frac{\Omega_{\mathrm{p}}(t)}{\Omega_{\mathrm{s}}(t)} = 0, \lim_{t\to\infty} \frac{\Omega_{\mathrm{p}}(t)}{\Omega_{\mathrm{s}}(t)} = \infty, \tag{8}$$

i.e. $\theta(-\infty) = 0$ and $\theta(+\infty) = \frac{\pi}{2}$, when the two pulses are applied in counterintuitive order. Moreover, in the adiabatic limit, we are allowed to neglect in Eq. (7) the term $[\boldsymbol{W}^{\mathrm{T}} \frac{\partial \boldsymbol{W}}{\partial t}, \rho^\alpha]$ so that it turns out to be

$$\mathrm{i}\,\hbar \frac{\partial \rho^\alpha}{\partial t} = [H^\alpha, \rho^\alpha] + \boldsymbol{W}^{\mathrm{T}} D \boldsymbol{W}, \tag{9}$$

with

$$[H^\alpha, \rho^\alpha] = \frac{\hbar}{2}\Omega \begin{pmatrix} 0 & \rho_{+-} & 2\rho_{+-} \\ -\rho_{0+} & 0 & \rho_{0+} \\ -2\rho_{-+} & -\rho_{-+} & 0 \end{pmatrix}. \tag{10}$$

Next we assume that the dephasing rates $\gamma_{12}$, $\gamma_{13}$, and $\gamma_{23}$ are much smaller than the Rabi frequencies $\Omega_{\mathrm{p0}}$ and $\Omega_{\mathrm{s0}}$. Within this weak dephasing approximation, the adiabatic basis presents a major advantage: coherences $\rho_{0+}$, $\rho_{0-}$ and $\rho_{+-}$ between the adiabatic states remain negligible throughout the excitation stage and may therefore be neglected. On the contrary, in the diabatic basis, coherence $\rho_{13}$ may reach significant values during the adiabatic population transfer and thus has to be taken into account. Taking the above into consideration, we finally arrive at the following simple dynamic equations

$$\begin{aligned}
\dot\rho_{++} &= \frac{1}{2}\cos^2\theta\left(\frac{1}{2}\Gamma_{32} - \Gamma_{21}\right)\rho_{++} \\
&\quad + \frac{1}{2}\sin^2\theta\Gamma_{32}\rho_{00} - \frac{1}{4}\cos^2\theta\Gamma_{32}\rho_{--}, \\
\dot\rho_{00} &= -\left(\sin^2\theta\Gamma_{32} + \frac{1}{2}\cos^2\theta\Gamma_{21}\right)\rho_{00} \\
&\quad + \frac{1}{2}\cos^2\theta\Gamma_{21}, \\
\dot\rho_{--} &= \frac{1}{4}\cos^2\theta\Gamma_{32}\rho_{++} + \frac{1}{2}\sin^2\theta\Gamma_{32}\rho_{00} \\
&\quad + \frac{1}{2}\cos^2\theta\left(\Gamma_{32} - \frac{1}{2}\Gamma_{21}\right)\rho_{--},
\end{aligned} \tag{11}$$

constrained by $\rho_{++} + \rho_{00} + \rho_{--} = 1$. With the initial conditions $\rho_{00}(-\infty) = 1$ and $\rho_{\mu\nu}(-\infty) = 0$ $(\mu\nu \neq 00)$, we further have $\rho_{++} = \rho_{--} = \frac{1}{2}(1 - \rho_{00})$.

Then the analytical solution for $\rho_{00}$ may be attained from Eq. (11) as

$$\begin{aligned}
\rho_{00} = {} & \mathrm{e}^{-\Gamma_{21}(\frac{t}{2}+T)}(1+\mathrm{e}^{\frac{4\tau}{T^2}t})^{\frac{(\Gamma_{21}-2\Gamma_{32})T^2}{8\tau}}\ (1+\mathrm{e}^{-\frac{8\tau}{T}})^{-\frac{(\Gamma_{21}-2\Gamma_{32})T^2}{8\tau}}\Bigg\{1+\mathrm{e}^{\Gamma_{21}(\frac{t}{2}+T)}(1+\mathrm{e}^{-\frac{8\tau}{T}})^{\frac{(\Gamma_{21}-2\Gamma_{32})T^2}{8\tau}} \\
& \times \mathrm{Hypergeometric2F1}\left[\frac{\Gamma_{21}T^2}{8\tau}, 1+\frac{\Gamma_{21}T^2}{8\tau}-\frac{\Gamma_{32}T^2}{4\tau}, 1+\frac{\Gamma_{21}T^2}{8\tau}, -\mathrm{e}^{\frac{4\tau}{T^2}t}\right] - (1+\mathrm{e}^{-\frac{8\tau}{T}})^{-\frac{(\Gamma_{21}-2\Gamma_{32})T^2}{8\tau}} \\
& \times \mathrm{Hypergeometric2F1}\left[\frac{\Gamma_{21}T^2}{8\tau}, 1+\frac{\Gamma_{21}T^2}{8\tau}-\frac{\Gamma_{32}T^2}{4\tau}, 1+\frac{\Gamma_{21}T^2}{8\tau}, -\mathrm{e}^{\frac{8\tau}{T^2}}\right]\Bigg\}.
\end{aligned} \tag{12}$$

Populations in the diabatic states $|1\rangle$, $|2\rangle$ and $|3\rangle$ can be determined from populations in the adiabatic states $|-\rangle$, $|0\rangle$ and $|+\rangle$ with Eq. (4) taken into account. After neglecting the coupling of coherences between the adiabatic states, populations in the diabatic states become

$$\begin{aligned}\rho_{11} &= \frac{1}{2}(1-\rho_{00})\sin^2\theta + \rho_{00}\cos^2\theta,\\ \rho_{22} &= \frac{1}{2}(1-\rho_{00}),\\ \rho_{33} &= \frac{1}{2}(1-\rho_{00})\cos^2\theta + \rho_{00}\sin^2\theta,\\ \rho_{13} &= \frac{1}{2}\frac{\mathrm{e}^{\frac{2\tau}{T^2}t}}{1+\mathrm{e}^{\frac{4\tau}{T^2}t}}|1-3\rho_{00}|. \end{aligned} \tag{13}$$

Equations (12) and (13) attained in the adiabatic limit are our main analytical results and will be used in the next section to demonstrate a few numerical plots of population and coherence evolution.

## 3. Results based on the analytical solutions

In this section, we explore the condition for obtaining the maximum coherence and population transfer between states $|1\rangle$ and $|3\rangle$ via the analytical solutions obtained in the last section. We first discuss the coherence between states $|1\rangle$ and $|3\rangle$

$$\rho_{13} = \frac{1}{2}\frac{\mathrm{e}^{\frac{2\tau}{T^2}t}}{1+\mathrm{e}^{\frac{4\tau}{T^2}t}}|1-3\rho_{00}| = A_{13}\rho_{130} \tag{14}$$

with $A_{13} = |1-3\rho_{00}|$ and $\rho_{130} = \frac{1}{2}\frac{\mathrm{e}^{\frac{2\tau}{T^2}t}}{1+\mathrm{e}^{\frac{4\tau}{T^2}t}}$. It is clear that, when the pulse width $T$ and the time delay $\tau$ are fixed, the factor $\rho_{130}$ depends only on time $t$ and reaches its maximum value $1/4$ at $t=0$. On the other hand, the factor $A_{13}$ depends on $\rho_{00}$ and its maximum value is 2 because $1 \geq \rho_{00} \geq 0$. Equation (12) shows that $\rho_{00}$ is sensitive to the spontaneous decay rates $\Gamma_{32}$ and $\Gamma_{21}$ as determined by a complicated hypergeometric function. When $\Gamma_{32}=0$, level $|3\rangle$ can be regarded as a steady state and we have $\rho_{00}=1$ and $\rho_{22}=0$ from Eq. (12) and Eq. (13). In particular, $\rho_{13}$ reaches its maximal value $1/2$ at $t=0$, which is a symbol of perfect STIRAP. To study the effects of $\Gamma_{32}$ and $\Gamma_{21}$ on coherence generation, we plot with Eq. (12) and Eq. (13) in Fig. 2(a) $\rho_{13}$ as a function of time $t$ with different values of the spontaneous decay rate $\Gamma_{32}$ and $\Gamma_{21}$. We can see that the plotted curves tend to form two separate groups corresponding to $\Gamma_{32}=10$ MHz and $\Gamma_{32}=50$ MHz, and the group for $\Gamma_{32}=10$ MHz is more compact than the group for $\Gamma_{32}=50$ MHz. This means that $\rho_{13}$ is less sensitive to $\Gamma_{21}$ than $\Gamma_{32}$, and $\Gamma_{21}$ has more influence on $\rho_{13}$ when $\Gamma_{32}$ is relatively large. Moreover, among the well separated curves, those corresponding to the larger $\Gamma_{21}$ are distinctly over those corresponding to the smaller $\Gamma_{21}$, which means that a bigger $\Gamma_{21}$ helps to compensate for the distructive effect of a bigger $\Gamma_{32}$. If we gradually increase $\Gamma_{32}$, $\rho_{13}$ will reach its maximum value (smaller than $1/2$) at a time other than $t=0$, and the maximal value of $\rho_{13}$ is mainly determined by $\Gamma_{32}$. For instance, the maximum value of $\rho_{13}$ is 0.45 at $t=-5.0$ ns when $\Gamma_{32}=10$ MHz while 0.35 at $t=-15$ ns when $\Gamma_{32}=50$ MHz.

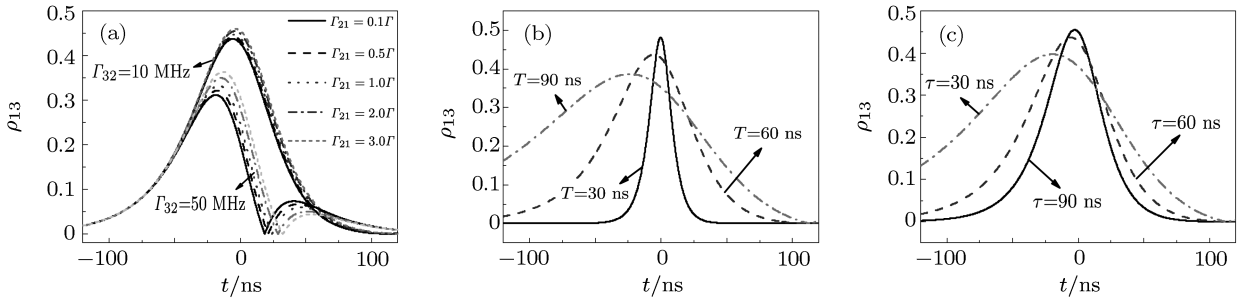



**Fig. 2.** Atomic coherence $\rho_{13}$ as a function of time $t$ with $T=60$ ns, $\tau=60$ ns and different spontaneous decay rates $\Gamma_{32}$ and $\Gamma_{21}$ (a); with $\tau=60$ ns, $\Gamma_{32}=10$ MHz, $\Gamma_{21}=38$ MHz, and different pulse widths $T$ (b); with $T=60$ ns, $\Gamma_{32}=10$ MHz, $\Gamma_{21}=38$ MHz, and different time delays $\tau$ (c). Other parameters are $\Omega_{\mathrm{p}0}=\Omega_{\mathrm{s}0}=400$ MHz, and $\Gamma=38$ MHz.

Then we discuss the influence of $T$ (pulse width) and $\tau$ (time delay) on $\rho_{13}$ (coherence between $|1\rangle$ and $|3\rangle$) with fixed spontaneous decay rates $\Gamma_{32}$ and $\Gamma_{21}$. As shown in Fig. 2(b), the peak value of $\rho_{13}$ declines slightly as the pulse width is increased from $T=30$ ns to 90 ns. Thus, the pulse width $T$ has similar influence on $\rho_{13}$ as the spontaneous decay rate $\Gamma_{32}$ because shortening the pulse width is equivalent to increas-

ing the spontaneous decay rate. On the other hand, Eq. (14) shows that $\tau$ is inversely proportional to $T^2$, i.e. an increase of the delay time is equivalent to narrowing the pulse width. In Fig. 2(c), we further show $\rho_{13}$ as a function of time $t$ with different values of time delay $\tau$. It is clear that the profile of $\rho_{13}(t)$ becomes thinner and thinner as $\tau$ is gradually increased and simultaneously the peak of $\rho_{13}(t)$ becomes higher and higher near $t = 0$.

Finally, we discuss how to achieve a large population transfer by modulating various parameters. From Eq. (13) we find that the initial conditions are $\rho_{00}(-\infty) = 1$, $\rho_{11}(-\infty) = 1$, $\rho_{22}(-\infty) = 0$, and $\rho_{33}(-\infty) = 0$. When $\Gamma_{32} = 0$, we have $\rho_{33}(\infty) = 1$ and $\rho_{11}(\infty) = 0$ and $\rho_{22} = 0$ at any time, i.e. the perfect STIRAP is accompanied with the largest population transfer. In the general case of $\Gamma_{32} \neq 0$, we have instead

$$\begin{aligned}
\rho_{11}(t) &= \frac{1}{2}(1-\rho_{00})\frac{1}{1+\mathrm{e}^{\frac{-4\tau}{T^2}t}} + \rho_{00}\frac{1}{1+\mathrm{e}^{\frac{4\tau}{T^2}t}},\\
\rho_{22}(t) &= \frac{1}{2}(1-\rho_{00}),\\
\rho_{33}(t) &= \frac{1}{2}(1-\rho_{00})\frac{1}{1+\mathrm{e}^{\frac{4\tau}{T^2}t}} + \rho_{00}\frac{1}{1+\mathrm{e}^{\frac{-4\tau}{T^2}t}} \qquad (15)
\end{aligned}$$

for the Gaussian pulses of the pump and Stokes lasers. Thus, after the atom–field interaction, the involved populations turn out to be

$$\rho_{11}(\infty) = \rho_{22}(\infty) = \frac{1}{2}(1-\rho_{00}), \qquad (16)$$

$$\rho_{33}(\infty) = \rho_{00}. \qquad (17)$$

As $\Gamma_{21}$ has little influence on $\rho_{00}$ (see Fig. 2(a)), we may assume that $\rho_{11}$, $\rho_{22}$ and $\rho_{33}$ have no relation with $\Gamma_{21}$, as indicated by Eq. (15).

In Fig. 3, we show populations $\rho_{11}$, $\rho_{22}$ and $\rho_{33}$ as functions of time $t$ with different spontaneous decay rates as well as different pulse widths and time delays. It is easy to find that the largest population transfer over 80% [see Fig. 3(b)] can be achieved even with spontaneous decay rates $\Gamma_{32} = 10$ MHz and $\Gamma_{21} = 38$ MHz when $T = 30$ ns and $\tau = 60$ ns. With $\Gamma_{32}$ increasing, the maximum value of $\rho_{33}$ is gradually reduced and its peak position approaches the $t = 0$ point more and more [see Figs. 3(a)] for a fixed delay $\tau$ and a fixed pulse width $T$. From Fig. 3(b) we can see that $\rho_{33}$ is gradually reduced in amplitude for a fixed spontaneous decay rate $\Gamma_{32}$ and a fixed delay $\tau$. This relation can be well explained by Eq. (12) and Eq. (15). As to the effect of the square of pulse width $T$ on $\rho_{33}$, it is inversely proportional to that of the spontaneous decay rate $\Gamma_{32}$. Figure 3(c) shows that the maximum value of $\rho_{33}$ increases and its peak position approaches the point $t = 0$ more and more with the increasing of time delay $\tau$ for a fixed spontaneous decay rate $\Gamma_{32}$ and a fixed pulse width $T$. Comparing Figs. 3(b) and 3(c), it is easy to find that the effect of $\tau$ is inversely proportional to that of $T^2$. Moreover, we can see that $\rho_{22} > 0$ when $T > 0$, which means that this process is not a perfect STIRAP.

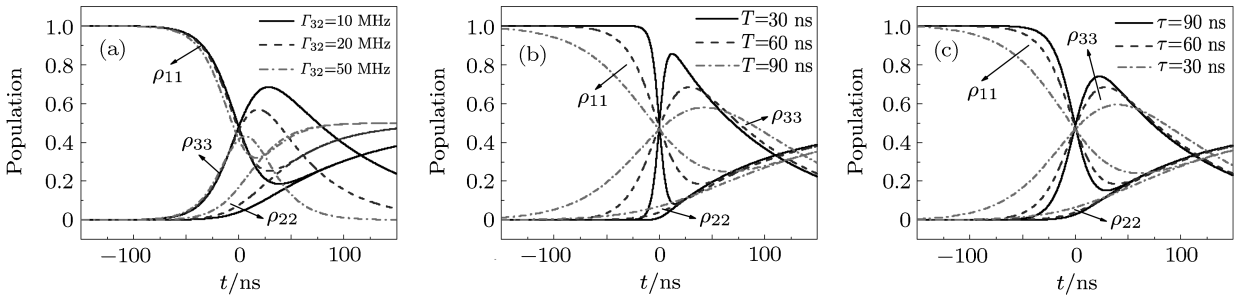



**Fig. 3.** Population $\rho_{11}$, $\rho_{22}$, and $\rho_{33}$ as a function of time $t$ with $T = 60$ ns, $\tau = 60$ ns and different spontaneous decay rates $\Gamma_{32}$ (a); with $\Gamma_{32} = 10$ MHz, $\tau = 60$ ns and different pulse widths $T$ (b); with $\Gamma_{32} = 10$ MHz, $T = 60$ ns and different time delays $\tau$ (c). Other parameters are $\Omega_{\mathrm{p}0} = \Omega_{\mathrm{s}0} = 400$ MHz and $\Gamma_{21} = 38$ MHz.

## 4. Results based on the numerical calculations

In this section, we examine the validity of the analytical solutions by full numerical calculations starting from Eq. (3) coupled with the Maxwell wave equations

$$\begin{aligned}
\frac{\partial \Omega_{\mathrm{p}}}{\partial z} + \frac{1}{c}\frac{\partial \Omega_{\mathrm{p}}}{\partial t} &= \mathrm{i}\,\kappa_{12}\rho_{21},\\
\frac{\partial \Omega_{\mathrm{s}}}{\partial z} + \frac{1}{c}\frac{\partial \Omega_{\mathrm{s}}}{\partial t} &= \mathrm{i}\,\kappa_{23}\rho_{32}. \qquad (18)
\end{aligned}$$

where

$$\kappa_{12} = \omega_{\mathrm{p}} N |d_{12}|^2 / 2\varepsilon_0 c\hbar$$

and

$$\kappa_{23} = \omega_{\rm s} N |d_{23}|^2 / 2\varepsilon_0 c\hbar$$

are the coupling constants, $N$ is the atomic density, $\varepsilon_0$ is the permittivity of the vacuum and $c$ is the speed of light in vacuum.

Assuming once again that both the pump and Stokes lasers are Gaussian pulses, we set $\Omega_{\rm s0} = \Omega_{\rm p0} = \Omega_0 = 400$ MHz to fulfil the condition of adiabatic evolution (1) and set appropriate time delay $\tau$ and pulse width $T$ to satisfy the condition of adiabatic evolution (2) in the weak dephasing approximation. In Fig. 4, we show coherence $\rho_{13}$ and populations $\rho_{11}$ and $\rho_{33}$ as a function of time $t$ with different values of several critical parameters. The solid curves correspond to analytical solutions while the dashed curves are obtained by full numerical calculations. We can see that there is only a small difference between the solid and dashed curves, i.e. the numerical solutions are in good agreement with the analytical solutions. It is worth emphasizing that we have $\Gamma_{32} = 3.0$ MHz if $^5{\rm P}_{3/2}$ and $^6{\rm D}_{1/2}$ of rubidium atoms are chosen as states $|2\rangle$ and $|3\rangle$, which is smaller than those in our calculations. This means that our calculations are universally significant and that the weak dephasing approximation is very accurate for the considered ladder system.

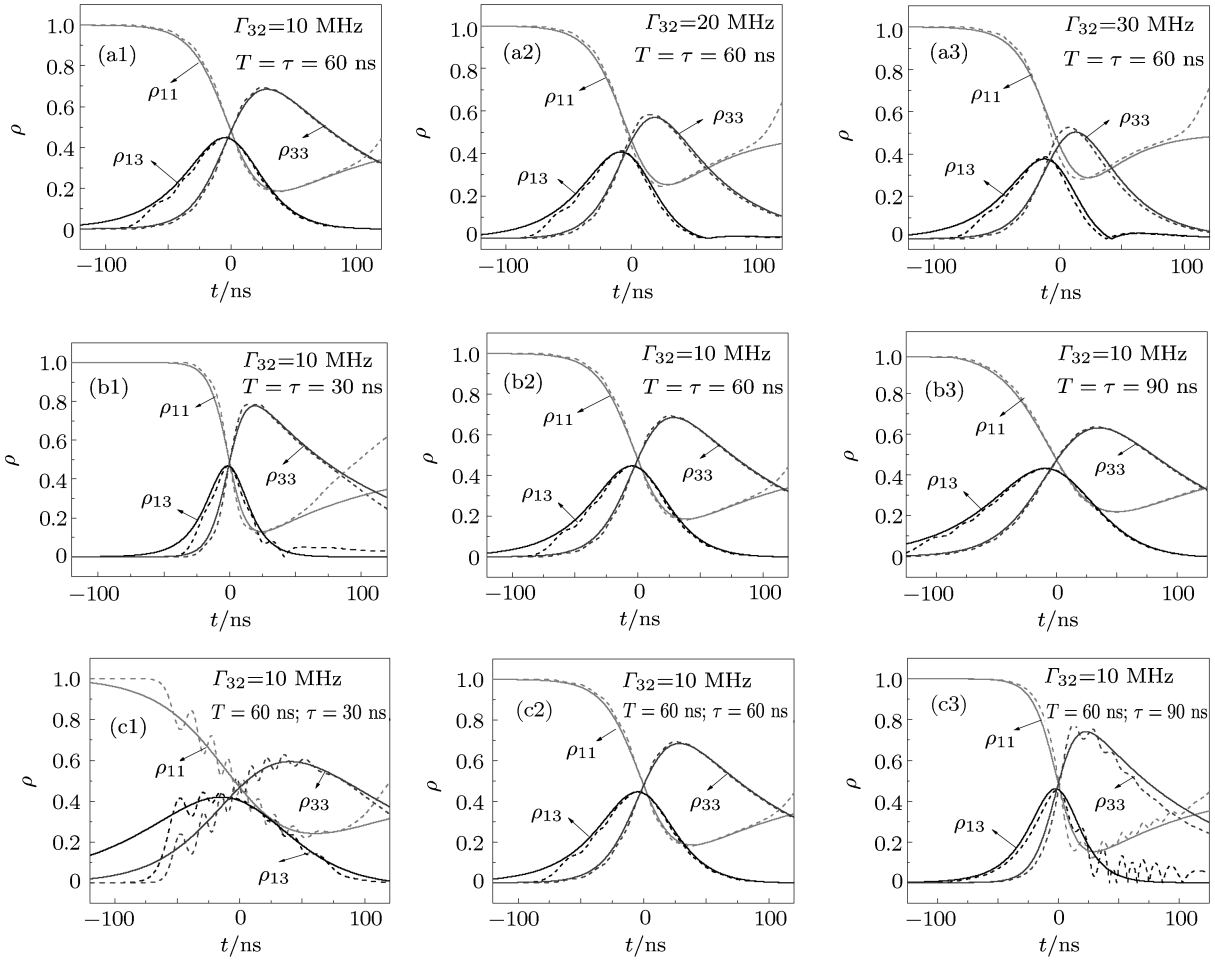



**Fig. 4.** Coherence $\rho_{13}$ and populations $\rho_{11}$ and $\rho_{33}$ as a function of time $t$ with different values of spontaneous decay rate $\Gamma_{32}$ (a); of pulse width $T$ (b); of time delay $\tau$ (c). Other parameters are $\Omega_{\rm p0} = \Omega_{\rm s0} = 400$ MHz and $\Gamma_{21} = 38$ MHz.

## 5. Conclusions

In summary, we have explored the effects of spontaneous decay rates $\Gamma_{21}$ and $\Gamma_{32}$, pulse width $T$ and time delay $\tau$ on the population transfer from state $|1\rangle$ to state $|3\rangle$ and related atomic coherence in a ladder-type atomic system. We have derived approximate analytical solutions from the expanded Liouville equations in the adiabatic limit and weak dephasing approximation, which are verified to be very accurate

by comparison with full numerical simulations. Our analytical and numerical results show that the large coherence and population transfer can be achieved by carefully modulating the pump and Stokes pulses, and the maximal value of coherence $\rho_{13}$ depends critically on the spontaneous decay rates and pulse width and time delay between the two laser pulses. In particular, the maximum value of coherence and population transfer decreases as $\Gamma_{32}$ becomes larger, it is not sensitive to $\Gamma_{21}$. To compensate for the destructive effect of spontaneous decay rates, one can reduce the pulse width $T$ and/or increase the pulse delay $\tau$ as long as the adiabaticity is maintained.

## References


[1] Vitanov N V, Halfmann T, Shore B W and Bergmann K 2001 *Rev. Phys. Chem.* **52** 763

[2] Payne M G and Deng L 2001 *Phys. Rev.* A **64** 031802

[3] Kozuma M, Akamatsu D, Deng L, Hagley E W and Payne M G 2002 *Phys. Rev.* A **66** 031801

[4] Wang H H, Du D M, Fan Y F, Li A J, Wang L, Wei X G, Kang Z H, Jiang Y, Wu J H and Gao J Y 2008 *Appl. Phys. Lett.* **93** 231107

[5] Payne M G and Deng L 2002 *Phys. Rev.* A **65** 063806

[6] Wang H H, Wang L, Wei X G, Li Y J, Du D M, Kang Z H, Jiang Y and Gao J Y 2008 *Appl. Phys. Lett.* **92** 041107

[7] Jain M, Xia H, Yin G Y, Merriam A J and Harris S E 1996 *Phys. Rev. Lett.* **77** 4326

[8] Wang L, Song X L, Li A J, Wang H H, Wei X G, Kang Z H, Jiang Y and Gao J Y 2008 *Opt. Lett.* **33** 2380

[9] Li A J, Song X L, Wei X G, Wang L and Gao J Y 2008 *Phys. Rev.* A **77** 053806

[10] Zhang B, Xu W H, Zhang H F and Gao J Y 2004 *Chin. Phys.* **13** 1722

[11] Jia G R , Ren Z Z, Wu S L and Zhang X Z 2009 *Chin. Phys.* B **18** 5272

[12] Li X H, Zhang X Z, Zhang R Z and Yang X D 2007 *Chin. Phys.* B **16** 2924

[13] Kis Z and Renzoni F 2002 *Phys. Rev.* A **65** 032318

[14] Ye C Y, Sautenkov V A, Rostovtsev Y V and Scully M O 2003 *Opt. Lett.* **28** 2213

[15] Remacle F and Levine R D 2006 *Phys. Rev.* A **73** 033820

[16] Gaubatz U, Rudecki P, Schiemann S and Bergmann K 1990 *J. Chem. Phys.* **92** 5363

[17] Bergmann K, Theuer H and Shore B W 1998 *Rev. Mod. Phys.* **70** 1003

[18] Vitanov N V, Fleischhauer M, Shore B W and Bergmann K 2001 *Opt. Phys.* **46** 55

[19] Broers B, van den Heuvell H B and Noordam L D 1992 *Phys. Rev. Lett.* **69** 2062

[20] Maas D J, Rella C W, Antoine P, Toma E S and Noordam L D 1999 *Phys. Rev.* A **59** 1374

[21] Rickes T, Yatsenko L P, Steuerwald S, Halfmann T, Shore B W, Vitanov N V and Bergmann K 2000 *J. Chem. Phys.* **113** 534

[22] Rangelov A A, Vitanov N V, Yatsenko L P, Shore B W, Halfmann T and Bergmann K 2005 *Phys. Rev.* A **72** 053403

[23] Xue Y, Wang G, Wu J H and Gao J Y 2007 *Phys. Rev.* A **75** 063832

[24] Sangouard N, Yatsenko L P, Shore B W and Halfmann T 2006 *Phys. Rev.* A **73** 043415

[25] Camp H A, Shah M H, Trachy M L, Weaver O L and DePaola B D 2005 *Phys. Rev.* A **71** 053401

[26] Yatsenko L P, Rangelov A A, Vitanov N V and Shore B W 2006 *J. Chem.Phys.* **125** 014302

[27] Almazor M L, Dulieu O, Elbs M, Tiemann E and Masnou-Seeuws F 1999 *Eur. Phys. J.* D **5** 237

[28] Fernandez R G, Ekers A, YatsenkoL P, Vitanov N V and Bergmann K 2005 *Phys. Rev. Lett.* **95** 043001

[29] Süptitz W, Duncan B C and Gould P L 1997 *J. Opt. Soc. Am.* B **14** 1001

[30] Ivanov P A, Vitanov N V and Bergmann K 2004 *Phys. Rev.* A **70** 063409

[31] Ivanov P A, Vitanov N V and Bergmann K 2005 *Phys. Rev.* A **72** 053412

[32] Band Y B 1992 *Phys. Rev.* A **45** 6643